

RESEARCH PAPER

Assessment of the rain drop inertia effect for radar-based turbulence intensity retrievals

ALBERT C.P. OUDE NIJHUIS¹, FELIX J. YANOVSKY², OLEG KRASNOV¹, CHRISTINE M.H. UNAL¹,
HERMAN W.J. RUSSCHENBERG¹ AND ALEXANDER YAROVY¹

A new model is proposed on how to account for the inertia of scatterers in radar-based turbulence intensity retrieval techniques. Rain drop inertial parameters are derived from fundamental physical laws, which are gravity, the buoyancy force, and the drag force. The inertial distance is introduced, which is a typical distance at which a particle obtains the same wind velocity as its surroundings throughout its trajectory. For the measurement of turbulence intensity, either the Doppler spectral width or the variance of Doppler mean velocities is used. The relative scales of the inertial distance and the radar resolution volume determine whether the variance of velocities is increased or decreased for the same turbulence intensity. A decrease can be attributed to the effect that inertial particles are less responsive to the variations of wind velocities. An increase can be attributed to inertial particles that have wind velocities corresponding to an average of wind velocities over their backward trajectories, which extend outside the radar resolution volume. Simulations are done for the calculation of measured radar velocity variance, given a 3-D homogeneous isotropic turbulence field, which provides valuable insight in the correct tuning of parameters for the new model.

Keywords: Radar applications, Radar signal processing and system modelling, Radar-based turbulence intensity retrievals

Received 1 November 2015; Revised 26 April 2016; Accepted 4 May 2016; first published online 9 June 2016

I. INTRODUCTION

In this paper the rain drop inertia effect is investigated and an improved radar forward model is proposed to enhance the accuracy of radar-based turbulence intensity retrievals when they are applied during precipitation. It can be relevant for research on atmospheric turbulence, with the possibility to improve remote measurements of turbulence intensity. A practical application is found in aviation where meteorological conditions and weather hazards have a significant impact on flight safety. That is why many airports in the world are equipped with weather radars that are used to alert for dangerous meteorological phenomena, in particular, zones of turbulence. Due to increasing intensity of flights, it is important to minimize the time between consecutive pairs of landing and/or taking off aircraft. From this point of view, wake vortices became one of the most important limiting factors of the airport capacity [1]. Therefore it is necessary to have a tool for predicting the behaviour of wake vortices: a wake vortex monitoring system [2]. While strong turbulence is dangerous by itself, very light or negligible turbulence plays an important role as it is associated with long wake vortex lifetimes [3]. When the turbulence intensity is measured it can be used to predict the duration of wake vortices [3].

Scanning radars and lidars are promising sensors for remote sensing of turbulence intensity and wind vectors, giving potential to the retrieval of the local atmospheric dynamics with high accuracy [4, 5]. A great advantage of such modern remote tools is the possibility to observe large volumes of the atmosphere with rather high resolution. Radars and lidars have the ability to work operationally in a collaborative way in different weather conditions like fog, precipitation, and dry air. For the observation of air motion both instruments are relying on the backscatter of particles, which randomly fills the observation volume and are involved in air motion. Typical backscatterers for radar are rain/cloud drops and ice crystals, and aerosols for lidar. Different scattering and attenuation mechanisms of light/infrared waves for lidar and of microwaves for radar result in the fact that the lidar is able to retrieve the eddy dissipation rate (EDR) remotely during clear sky conditions and the radar is able to do the same in presence of clouds or precipitation [6–8].

The turbulence intensity, quantified by the EDR, is one of the fundamental parameters used to describe turbulence characteristics, see e.g. Pope [9]. The EDR represents the rate at which energy from large scales cascades to smaller eddies until the energy is transformed to heat. EDR is one of the key parameters in numerical models for balancing the energy budget of the atmosphere. Knowledge of the EDR in the troposphere is also important for understanding the thermal and dynamical structures as well as studying the mixing of minor constituents such as air pollutants. The variance of the mean Doppler velocities can be used to retrieve the EDR [10, 11]. This approach was implemented using

¹Delft University of Technology, Delft, the Netherlands

²National Aviation University, Kiev, Ukraine

Corresponding author:

A.C.P. Oude Nijhuis

Email: albertoudenijhuis@gmail.com

vertically-pointing lidar by O'Connor *et al.* [12]. At the Hongkong international airport, nowadays operational turbulence monitoring is done by mapping the EDR field with a scanning lidar [13].

In this paper we focus on radar based retrieval techniques of turbulence intensity using the Doppler spectral width (DSW), which is used in several algorithms [14–18]. In recent years the radar-based estimation of the rainfall rate has improved by making use of a simultaneous retrieval of the drop size distribution (DSD) for radars with a low elevation angle [19]. Also a retrieval technique from a slant looking radar has been developed to retrieve the DSD [20]. However an accurate estimation and validation of turbulence intensity during precipitation by using the radar has not received a lot of attention. The rain DSD can be an essential input to radar-based EDR retrieval techniques to improve accuracy of the resulting turbulence intensity [11]. The rain DSD parameters can for example be estimated from polarimetric parameters [21]. In spite of essential progress achieved, EDR retrieval techniques are nowadays not accurate enough for many applications. One point of concern is the impact of the rain drops inertia when Doppler radar measurements are used for turbulence estimation. This point is investigated, theoretically and by simulations in this paper.

One of the most difficult issues related with accurate retrieval of EDR from the scattered signal is taking into account the inertia of the scatterers. Actually the echo-signal is scattered from particles that are located in the resolution volume but not from the turbulence itself. The first works supposed that the scatterers are able to follow turbulent eddies perfectly; this is true for very small particles such as aerosols that are relevant for the lidar, it is almost true for dry snowflakes [22] but is rather doubtful for rain drops. It is rather obvious that larger droplets are less effective as the tracers of the air motion; but how to estimate this quantitatively? And how to use it in radar models to improve the results of turbulence intensity retrieval?

An approach was proposed by Yanovsky [23] and it is used in [11, 24]. This approach takes into account that atmospheric turbulence is a complex vortical motion with a spectrum of spatial scales of eddies. The larger scales have more energy at the same EDR. The authors introduce a bounded deterministic function, which describes the relationship between the drop size diameter D and the level of involvement of the droplet for a given size into the motion of a given scale. This approach is based on four suppositions: (1) for each drop size there is a minimum length scale L_{min} ; (2) for turbulent motions larger than L_{min} the drop is a perfect tracer; (3) for turbulent motions smaller than L_{min} the drop will not participate in the motion; (4) for $L_{min} = f(D)$, the approximation was introduced based on estimations of the droplet relaxation times. The approach of Yanovsky [23] is based on heuristic suppositions that are rather flexible and allows adaption of the model to a real situation. Nevertheless, it is much better to have an algorithm based on fundamental laws of physics, which are the equations of motions for a rain drop. In this paper a correction for rain drop inertia is developed, that is necessary for radar-based turbulence intensity retrievals during rain. First rain drop inertial parameters are derived from the equations of motion of a rain drop. In this work we reuse existing theoretical and experimentally validated work regarding the equations of motion for a rain drop form Khvorostyanov and Curry [25]. In contrast to

Khvorostyanov and Curry [25] that used these equations for the estimation of rain drop terminal fall speeds, in this work these equations are used to estimate rain drop inertial parameters.

The paper is structured as follows. In Section II we derive particle inertial parameters from fundamental physical laws. In Section III, a new model is described that is able to account for the inertia effect. In Section IV tuning parameters of the model are obtained by using a stochastic three-dimensional (3-D) homogeneous isotropic turbulence model. In Section V, mathematical relations are given that show how the model for inertia correction can be implemented in a radar retrieval technique. And in the end conclusions are drawn.

II. RAIN DROP INERTIAL PARAMETERS

In this section we aim at finding rain drop inertial parameters, which quantify how much a particle behaves as a perfect tracer or, alternatively speaking, how much a scatterer responds to fluctuations in wind velocities throughout its trajectory. To obtain rain drop inertial parameters that can be used in radar-based retrieval techniques for the estimation of EDR from the DSW, it makes sense to start from fundamental physics, which are the equations of motion for a rain drop. However the problem is that the equations of motions cannot be applied directly in a retrieval algorithm because only limited information is available. Therefore it is necessary to simplify the equations of motion down to scalars, the inertial parameters that can represent the behavior of an ensemble of particles. The advantage of this approach is that it is possible to verify all model assumptions and better adapt this approach to specific applications. In addition the same procedure can be applied to other classes of hydrometeors such as ice crystals. Works with such a fundamental approach already exist. Khvorostyanov and Curry [25] started from the equations of motion for drop/ice particles and successfully estimated their terminal fall speeds. One of the most difficult parts in such works is the determination of the drag force coefficient for rain drops and ice particles. Here we reuse existing work from Khvorostyanov and Curry [25] but now with the aim of estimating inertial parameters instead of the terminal fall speed. The equations of motion using the Cartesian coordinate system for a particle in the x/y - and z -direction can be written as:

$$\frac{dv_{p,xy}}{dt} = \frac{\pm F_{d,xy}}{m} = \mp \eta_{xy}(v_{a,xy} - v_{p,xy})^2, \quad (1)$$

$$\frac{dv_{p,z}}{dt} = \frac{-F_g + F_b \pm F_{d,z}}{m} = -\eta_z v_t^2 \mp \eta_z(v_{a,z} - v_{p,z})^2, \quad (2)$$

with

$$\eta_{xy} = \frac{\rho_F A_{xy} C_{d,xy}}{2m}, \quad \eta_z = \frac{\rho_F A_z C_{d,z}}{2m}, \quad (3)$$

where $v_{p,*}$ is the particle velocity, $v_{a,*}$ air velocity, v_t the terminal particle fall speed, $F_{d,*} = 1/2 \rho_F A_* C_{d,*} (v_{a,*} - v_{p,*})^2$ the drag force, ρ_F the air density, A_* the projected particle

surface area in direction $*$, $C_{d,*}$ the drag force coefficient, $F_g = mg$ gravity, m the particle mass, g the gravitational acceleration and $F_b = \rho_F V_b g$ buoyancy force and V_b the volume of the particle. Here η_z [m^{-1}] and η_{xy} [m^{-1}] are scalars to write the equations of motion in a brief way. The calculations for the drag force coefficients $C_{d,*}$ are extensive and can be obtained from the work of Khvorostyanov and Curry [25]. For rain drops in the air the buoyancy force can be neglected, as the gravitational force is much larger [25]. However, for crystallized ice particles, which can have much lower mass densities, the buoyancy force should also be considered. The direction of the drag force is opposite to the particle motion with respect to its surrounding air motion, which determines the right sign in the equations. For the remainder of this paper the terminal fall velocities and scalars η_{xy} and η_z are obtained from the work of Khvorostyanov and Curry [25]. As big rain drops have a spheroidal shape, also an axis ratio formula as a function of equivolumetric spherical drop diameter is used from Beard and Chuang [26]. When there is a balance between the gravitational, drag and buoyancy forces, the drop terminal fall speed is obtained as [25]:

$$v_t(D) = \left[\frac{2(|mg - F_b|)}{\rho_F A_z C_{D,z}} \right]^{1/2}, \tag{4}$$

where D is the equivolumetric spherical drop diameter. The total particle velocity can be written as:

$$\vec{v}_p = \vec{v}_t + \vec{v}_a + \vec{v}'_p, \tag{5}$$

where \vec{v}_t is the particle terminal fall velocity, \vec{v}_a is the air velocity and \vec{v}'_p the additional velocity difference due to relaxation. The direction of the terminal fall velocity is always in the negative z -direction, pointing towards the earth. The direction and magnitude of \vec{v}'_p can be obtained by numerically integrating the equations of motions, equations (1) and (2).

From analytical solutions to simple cases it is possible to estimate typical numbers that characterize the motion of an ensemble of particles. One of such simple cases is a sudden jump in velocity, from which a response time can be estimated. For the x/y -direction, the ‘‘sudden jump’’ case can be formulated as:

$$v_{a,xy} = \begin{cases} v_{a,xy}(-\infty) & \text{for } t < 0 \\ v_{a,xy}(\infty) & \text{for } t > 0 \end{cases}, \tag{6}$$

i.e. a step function at $t = 0$, for which the solution for the particle velocity at $t > 0$ is:

$$v_{p,xy}(t) = v_{a,xy}(\infty) + \frac{1}{1/[v_{a,xy}(-\infty) - v_{a,xy}(\infty)] - \eta_{xy}t}. \tag{7}$$

From the analysis of the ‘‘sudden jump’’ case we can define the inertial time for the x/y -direction $\tau_{I,xy}$ as the time that is required such that the relative difference in velocity has decreased with $\exp(-1)$:

$$\frac{v_{p,xy}(t) - v_{a,xy}(\infty)}{v_{a,xy}(-\infty) - v_{a,xy}(\infty)} = \exp(-1), \tag{8}$$

from which follows:

$$\tau_{I,xy} = \frac{1 - \exp(-1)}{\exp(-1)\eta_{xy}[v_{a,xy}(\infty) - v_{a,xy}(-\infty)]}. \tag{9}$$

It should be mentioned that such an inertial time is only a figure of merit and the reality is more complex. For the z -direction no analytical solution was found for the ‘‘sudden jump’’ case. It is however possible to find analytical solutions for more specific cases where the terminal fall speed is large or small compared with the order of magnitude of velocity differences due to relaxation $\mathcal{O}(v'_p)$. For the first case with a small terminal fall speed, i.e. $v_t \ll \mathcal{O}(v'_p)$, the solution is similar for the x/y -direction and the inertial time $\tau_{I,z1}$ is:

$$\tau_{I,z1} = \frac{1 - \exp(-1)}{\exp(-1)\eta_z[v_{a,z}(\infty) - v_{a,z}(-\infty)]}. \tag{10}$$

In case the terminal fall speed is large, i.e. $v_t \gg \mathcal{O}(v'_p)$, the equation of motion for the z -direction can be written as:

$$\frac{dv_{p,z}}{dt} = \frac{dv'_{p,z}}{dt} \approx \mp 2\eta_z v_t v'_{p,z} = \mp \frac{v'_{p,z}}{\tau_{I,z2}}, \tag{11}$$

with:

$$\tau_{I,z2} = \frac{1}{2\eta_z v_t}, \tag{12}$$

where $\tau_{I,z2}$ is the inertial time for the z -direction. Again the sign is such that the relaxation velocity, $v'_{p,z}$, is reduced, e.g. negative derivative, $dv'_{p,z}/dt$, when $v'_{p,z}$ is positive. For the ‘‘sudden jump’’ case the analytical solution is:

$$v_{p,z}(t) = -v_t + v_{a,z}(\infty) + [v_{a,z}(-\infty) - v_{a,z}(\infty)] \exp\left(-\frac{t}{\tau_{I,z2}}\right). \tag{13}$$

Given the inertial times, it is also possible now to approximate the inertial distances by assuming that the particles are moving with the terminal fall speed in the z -direction for $v_t \gg \mathcal{O}(v'_p)$, or otherwise moving with the final speed $v_{a,z}(\infty) - v_{a,z}(-\infty)$. The inertial distances are given in combination with an overview of all inertial parameters for rain drops in Table 1. Calculated values for the inertial distance are shown in Fig. 1. The inertial distance increases rapidly with the drop size. For large terminal fall speeds, $v_t \gg \mathcal{O}(v'_p)$, the inertia parameters are reduced. In Fig. 1 the calculated inertial parameters are also calculated for spherical drops, which shows that the spheroidal shape has only a minor impact. From the equations of motions for a rain drop inertial parameters have now been estimated by making several assumptions. Without any additional information, the derived inertial parameters give a best guess for the time (distance) that a particle needs to respond to a change in the wind field. These assumptions include the simplification of the equations of motion to analytical solutions to the ‘‘sudden jump’’ case. The analytical solutions are different for direction, either x/y or z , and in case of the z -direction the solutions deviate for relatively large or small terminal fall speeds. An additional assumption is made that the particle maintains its shape, i.e. no microphysics (evaporation/

Table 1. Inertial parameters for rain drops.

Direction	Inertial time	Inertial distance
x/y	$\tau_{I,xy} = \frac{1 - \exp(-1)}{\exp(-1)\eta_{xy}[v_{a,xy}(\infty) - v_{a,xy}(-\infty)]}$	$d_{I,xy} \approx \frac{1 - \exp(-1)}{\exp(-1)\eta_{xy}}$
$z, v_t \ll \mathcal{O}(v'_p)$	$\tau_{I,z1} = \frac{1 - \exp(-1)}{\exp(-1)\eta_z[v_{a,z}(\infty) - v_{a,z}(-\infty)]}$	$d_{I,z1} \approx \frac{1 - \exp(-1)}{\exp(-1)\eta_z}$
$z, v_t \gg \mathcal{O}(v'_p)$	$\tau_{I,z2} = \frac{1}{2\eta_z v_t}$	$d_{I,z2} \approx \frac{1}{2\eta_z}$

condensation) and no vibrations are considered. Although such simplifications are rather crude, they are necessary for the development of a radar forward model that can be used in retrievals, where information is the limiting factor.

III. A NEW MODEL FOR INERTIA CORRECTION

Here we propose a new way on how to account for the inertia of rain droplets, that can be used in radar forward models of the radar Doppler spectrum or the radar DSW. The proposed method provides a correction for the observed variance of Doppler velocities, given the equivolumetric drop size or DSD and the observed radar resolution volume parameters.

In the case of homogeneous isotropic turbulence, the Kolmogorov hypothesis [27] states that within the inertial subrange the statistical representation of the turbulent energy spectrum $S(k)$ is given by:

$$S(k) = C\epsilon^{2/3}k^{-5/3}, \tag{14}$$

where C is a Kolmogorov constant, ϵ the EDR and k the wavenumber. The variance of velocities, σ^2 , is then obtained as:

$$\sigma^2 = \int_{k_{min}}^{k_{max}} S(k)dk = \frac{3}{2}C\epsilon^{2/3}[k_{min}^{-2/3} - k_{max}^{-2/3}], \tag{15}$$

where k is the wavenumber that is related to a length scale L via $k = 2\pi/L$. This leads to the proportionality between the variance of velocities and length scales:

$$\sigma^2 \propto [L_{max}^{2/3} - L_{min}^{2/3}]. \tag{16}$$

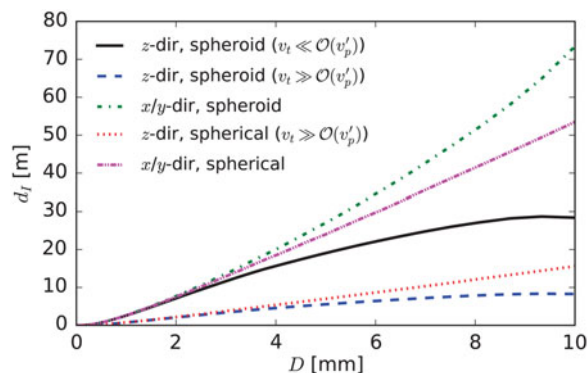


Fig. 1. The inertial distance d_I for rain drops is plotted as function of drop equivolumetric diameter D . The calculations are done both for spherical as spheroid droplets, for which the axis ratio relation from Beard and Chuang [26] is used. Note that “z-dir, spherical, $v_t \ll \mathcal{O}(v'_p)$ ” is not in the figure because it is the same solution as “x/y-dir, spherical”.

A correction ζ to the variance due to turbulence intensity, equation (16), can now be defined, which can be directly applied to the radar DSW:

$$\zeta = \sigma_{inertia} / \sigma_{no,inertia}, \tag{17}$$

where $\sigma_{inertia}$ is the standard deviation of velocities for the inertial particles and $\sigma_{no,inertia}$ is the standard deviation of velocities as if there was no inertia. Typically in a radar retrieval algorithm $\sigma_{inertia}$ is measured and one would like to have $\sigma_{no,inertia}$, which can be directly related to the turbulence intensity. The term $\sigma_{no,inertia}$ is related to perfect tracers of the air, as if the radar was looking to particles that were following the air motion exactly.

Based on equation (16) and the derived inertial parameters (Table 1) a new inertia correction model is proposed. The concept of the correction is twofold. Given a radar resolution volume scale L^* , both the maximal and the minimal scale for which the inertial particles are sensors are adjusted. The maximum scale is adjusted, as an ensemble of inertial particles can have more variations of velocities that are representative for a larger volume than the radar resolution volume. To do this a typical distance is defined, $d_{I,xyz}$, which is a 3-D distance on which the particle responds to variations in the wind field. On the other side, the inertial particles need a certain distance to respond to variations in the wind velocity, and also the smallest scale is adjusted. The inertia correction model can then be formulated as:

$$d_{I,xyz} = \sqrt{2^*d_{I,xy}^2 + d_{I,z2}^2}, \tag{18}$$

$$\zeta_{xy}^2(L_{xy}, D) = \frac{(L_{xy} + \alpha_{xy}d_{I,xyz})^{2/3} - (\beta_{xy}d_{I,xy})^{2/3}}{L_{xy}^{2/3}}, \tag{19}$$

$$\zeta_z^2(L_z, D) = \frac{(L_z + \alpha_zd_{I,xyz})^{2/3} - (\beta_zd_{I,z2})^{2/3}}{L_z^{2/3}}, \tag{20}$$

where L^* is the radar resolution volume scale for direction $*$ and $d_{I,xyz}$ is 3-D inertial distance. Here we introduce α^* and β^* , which are dimensionless tuning parameters that can be used to adapt this model based on additional information such as simulations or experiments. Note that for ($\alpha^* = 0, \beta^* = 0$) the result is that $\zeta = 1$ and there is no correction. Here we choose $d_{I,z2}$, i.e. the solution for $v_t \gg \mathcal{O}(v'_p)$, which seems legitimate for small turbulence intensities in precipitation. The alternative, $d_{I,z1}$, has a similar dependency on D , which can be seen in Fig. 1. Estimated uncertainties in α^* and β^* from simulations or experiments should be able to

cover for such an introduced uncertainty. In Fig. 2 the model for inertia correction is shown for different adaptation parameters α^* and β^* for a drop of 0.5 mm, which demonstrates both effects. The parameter α^* determines the importance of the correction for large scales. In Fig. 2 it can be seen that an increased value of α^* leads to an increased value of $\sigma_{inertia}$, which can be attributed to the “transport of velocity fluctuations” in the radar resolution volume. The parameter β^* determines the relative importance of the classical inertia effect, i.e. the limited response to the small scale velocity fluctuations. In Fig. 2 it can be seen that an increased value of β^* leads to a decrease in the value of $\sigma_{inertia}$, which can be interpreted as little (/no) response of inertial particles to small scale fluctuations.

The correction for any radar line of sight, relevant for application, with radar elevation θ is:

$$\zeta^2(L_{xy}, L_z, D, \theta) = \cos^2(\theta)\zeta_{xy}^2(L_{xy}, D) + \sin^2(\theta)\zeta_z^2(L_z, D). \tag{21}$$

IV. SIMULATIONS OF RAIN DROP INERTIA

In this section we show how wind field simulations can be used to adapt the model for inertia correction. A 3-D homogeneous isotropic turbulence model from Mann [28] is used to estimate the adaptation parameters α^* and β^* in the inertia correction model (equation (19) and (20)). The simulated wind field and the terminal fall speed of droplets can be used to calculate backward trajectories of rain drops. Given the backward trajectories, the additional velocity difference due to relaxation can then be calculated by implicit integration of the equations of motion. The additional velocity difference due to relaxation, i.e. the inertia effect, can then be used to estimate the difference in variance of Doppler velocities within a radar resolution volume. The simulations will also give an idea of the uncertainties of EDR estimation from the DSW due to the inertia effect.

Here we use the work of Mann [28] to obtain a 3-D homogeneous isotropic turbulence periodic field with spatial scales of $30 \times 30 \times 30 \text{ m}^3$, a spatial resolution of 1.2 m and an EDR

of $0.01 \text{ m}^2 \text{ s}^{-3}$, which is a typical value of daytime atmospheric EDR. The scale of 30 m is chosen because this is a typical maximum distance where inertia becomes less important (see Fig. 1). The parameters in the wind field simulation are chosen such that the simulated wind field satisfies the Kolmogorov energy spectrum for the inertial subrange, equation (14). Details of such simulations can be found in Mann [28]. The simulated wind fields are shown in the background of Fig. 3. Given the terminal particle velocity, the wind field and the assumption of no inertia, $\vec{v}'_p = 0$ in equation (5), the backward trajectories of particles can then be calculated. In Fig. 3 it can be seen that for small rain droplets (0.01 and 0.1 mm) the trajectories and the origins have a random nature, whereas for larger rain drops (0.5 and 4 mm) the trajectories have an orchestrated nature and the drops mainly originates from above.

To estimate the effect of inertia on the radar DSW, the following method is applied. On a line, either parallel to the x -direction or the z -direction, at a random position in the simulation, 100 equidistant points are taken for which the radar Doppler velocities are calculated, see Fig. 3. For the Doppler velocities the projected velocities in the line of sight are taken, e.g. u for the x -direction. Consequently the standard deviation of the Doppler velocities is calculated two times, with and without the velocity difference due to relaxation $v'_{p,*}$. The standard deviations can be used to calculate the inertia factor $\zeta_{*,i}$ for direction *, which is specific for the realization of this wind field and specific for the random location of the line spanning 100 equidistant drop locations for simulation number i :

$$\zeta_{*,i} = \sigma_{inertia} / \sigma_{no,inertia}, \tag{22}$$

where $\sigma_{inertia}$ is the standard deviation of line of sight velocities with $v'_{p,*}$ included. For $\sigma_{no,inertia}$ the relaxation term $v'_{p,*}$ is not included. An ensemble of such calculations can then be used to calculate optimal parameters in the model for inertia correction and to estimate the uncertainty in EDR from the DSW due to rain drop inertia.

For the estimation of the rain drop inertia effect, the velocity difference due to relaxation $v'_{p,*}$ needs to be calculated. First a backward trajectory is calculated, under the assumption that $v'_{p,*}$ is not too large and has a negligible influence on the

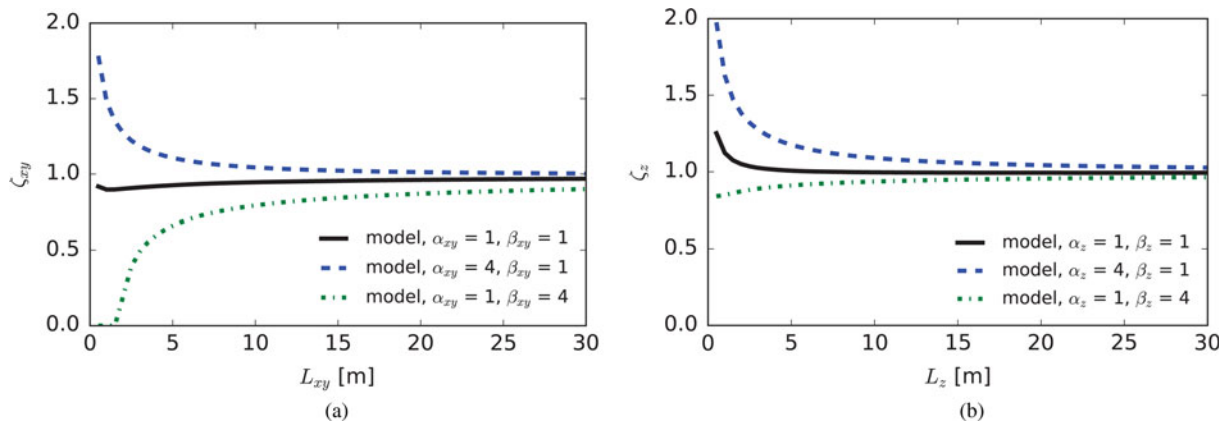


Fig. 2. The inertia correction ζ is plotted as a function of the observation length scale L^* for the direction * which is either x/y or z for a droplet with a diameter of $D = 0.5 \text{ mm}$. The plots are for different tuning parameters α^* and β^* . (a) $D = 0.5 \text{ mm}$, x/y -direction (b) $D = 0.5 \text{ mm}$, z -direction.

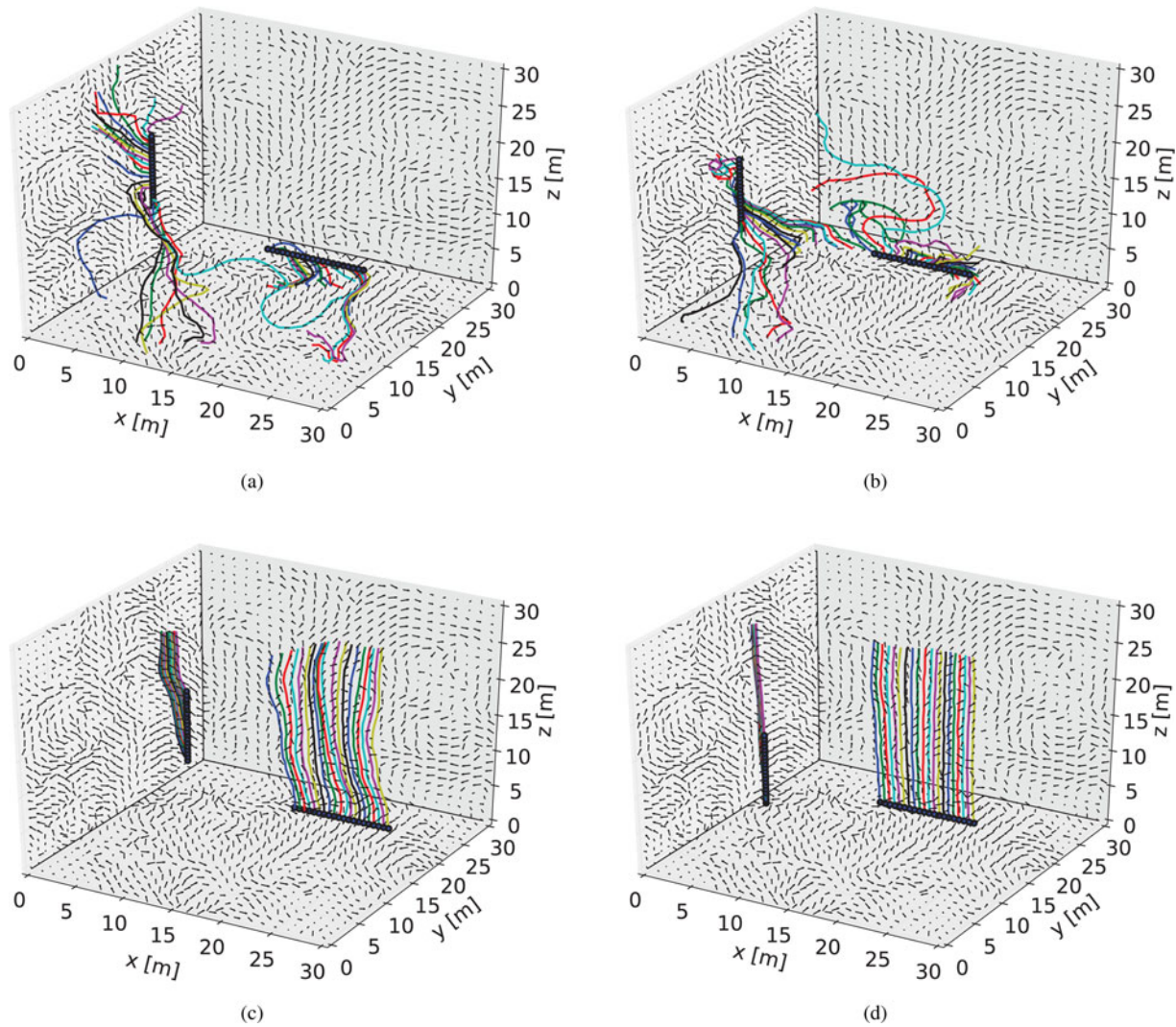


Fig. 3. Backward trajectories of rain drops are shown for different equivolumetric drop sizes D for the same 3-D wind field. The black dots represent the final locations of the drops, which are used in the simulations. In the background wind vectors used for the calculations are shown on the xy , xz , and yz -planes of a 3-D wind field simulation [28]. (a) $D = 0.01$ mm (b) $D = 0.1$ mm, (c) $D = 0.5$ mm (d) $D = 4$ mm.

trajectory. An advantage of this assumption is that the final position is not altered. Consequently the equations of motions are integrated over the trajectory to find the particle velocity difference due to relaxation $v'_{p,*}$. The equations of motion, equations (1) and (2), can be used to write the differential equations that describe the evolution of the relaxation term $v'_{p,*}$:

$$\frac{dv'_{p,xy}}{dt} = \begin{cases} +\eta_{xy} v'^2_{p,xy} & \text{for } v'_{p,xy} < 0 \\ -\eta_{xy} v'^2_{p,xy} & \text{for } v'_{p,xy} > 0 \end{cases} \quad (23)$$

$$\frac{dv'_{p,z}}{dt} = \begin{cases} +\eta_z [v'^2_{p,z} - 2v_t v'_{p,z}] & \text{for } v'_{p,z} < 0 \\ -\eta_z [v'^2_{p,z} - 2v_t v'_{p,z}] & \text{for } 0 < v'_{p,z} < \frac{v_t}{2} \\ +\eta_z [-2v_t^2 + 2v_t v'_{p,z} - v'^2_{p,z}] & \text{for } v'_{p,z} > \frac{v_t}{2} \end{cases} \quad (24)$$

Implicit integration of the differential equation:

$$\frac{dy}{dt} = ay^2 + by + c, \quad (25)$$

has the following solution:

$$y_{i+1} = -\frac{b}{2a} + \frac{1}{2a\Delta t} \pm \sqrt{\left(\frac{b}{2a} - \frac{1}{2a\Delta t}\right)^2 - \frac{y_i + c\Delta t}{a\Delta t}}, \quad (26)$$

which can be applied to find the following solutions of equations (23) and (24):

$$v'_{p,xy,i+1} = \begin{cases} +Q_1 - \sqrt{Q_1^2 + Q_2} & \text{for } U_{xy,i} < 0 \\ -Q_1 + \sqrt{Q_1^2 + Q_2} & \text{for } U_{xy,i} > 0 \end{cases}, \quad (27)$$

$$v'_{p,z,i+1} = \begin{cases} +Q_3 - \sqrt{Q_3^2 + Q_4} & \text{for } U_{z,i} < 0 \\ -Q_3 + \sqrt{Q_3^2 + Q_4} & \text{for } 0 < U_{z,i} < \frac{v_t}{2} \\ -Q_3 + \sqrt{Q_3^2 + Q_5} & \text{for } U_{z,i} > \frac{v_t}{2} \end{cases}, \quad (28)$$

with

$$U_{xy,i} = v_{a,xy,i+1} - (v'_{p,xy,i} + v_{a,xy,i}), \quad (29)$$

$$U_{z,i} = v_{a,z,i+1} - (v'_{p,z,i} + v_{a,z,i}), \quad (30)$$

$$Q_1 = \frac{1}{2\eta_{xy}\Delta t}, \quad Q_2 = \left| \frac{U_{xy,i}}{\eta_{xy}\Delta t} \right|, \quad (31)$$

$$Q_3 = v_t + \frac{1}{2\eta_z\Delta t}, \quad Q_4 = \left| \frac{U_{z,i}}{\eta_z\Delta t} \right|, \quad Q_5 = Q_4 - 2v_t^2. \quad (32)$$

Given the terminal fall speed v_p , rain drop parameters to calculate η_* and a 3-D wind field simulation is it now possible to integrate the relaxation term $v'_{p,*}$. Typically it is necessary to integrate over a distance on the order of several $d_{l,xyz}$ to obtain a stable solution.

The results of the inertia correction factors $\zeta_{*,i}$ that are calculated from the simulations are shown in Fig. 4. On the x -axis the length scale L_* is varied, which defines the total distance of the line that spans the rain drop locations. On the y -axis the rain drop inertia correction factor is shown. Simulations are done for multiple drop sizes and for different looking directions (x and z). In Figs 4(e) and 4(f) it can be seen that for larger droplets the correction becomes more important as it deviates more from 1. The smaller the spatial scale L_* , i.e. shorter radar resolution volume scale/higher spatial radar resolution, the more important the inertia correction becomes. With a minimization of a cost function (Nelder-Mead Simplex) for the inertia correction ζ , it is possible to obtain optimal parameters for α_* and β_* which are summarized in Table 2. The minimization is executed separately for the x - and z -directions, and for different drop sizes. In addition the optimization of inertial parameters is done for all the drop sizes at the same time. The Root Mean Square Error (RMSE) in ζ increases for larger droplets, which can be expected as large rain droplets behave more as inertial particles. In Fig. 4

Table 2. Optimized tuning parameters α_* and β_* for the inertia correction model for rain drops with various diameters.

D (mm)	α_{xy}	β_{xy}	RMSE of ζ
0.10	0.56	0.00	1.08×10^{-3}
0.50	2.21	0.00	9.22×10^{-2}
4.00	585.68	657.55	1.94×10^0
all	273.57	263.77	8.11×10^{-1}
D (mm)	α_z	β_z	RMSE of ζ
0.10	-0.20	0.00	5.34×10^{-4}
0.50	0.14	0.00	1.45×10^{-2}
4.00	1.48	0.00	3.36×10^{-1}
all	2.59	2.64	1.21×10^{-1}

it can be seen that the model is sufficiently adaptable for the different cases. Especially for large droplets (e.g. 4 mm) and high resolution $L < 10$ m the uncertainties become very large.

V. RADAR FORWARD MODEL

In this section the mathematical equations are given that are related to the calculation of the radar observables that can be used in a retrieval of the turbulence intensity. Here it is accounted for the fact that the contributions to the radar spectral width due to the terminal fall speed of droplets and turbulence are not independent. This issue is discussed in e.g. Fang and Doviak [29]. The Doppler mean fall velocity v_D and DSW σ_D can be calculated as a sum over rain drop sizes:

$$v_D = \sum_i N(D_i)\sigma(D_i)v_f(D_i) \sin \theta / \sum_i N(D_i)\sigma(D_i), \quad (33)$$

$$\sigma_D^2 = \frac{\sum_i N(D_i)\sigma(D_i)[\zeta^2(D_i)\sigma_T^2 + (v_f(D_i) \sin \theta - v_D)^2]}{\sum_i N(D_i)\sigma(D_i)}, \quad (34)$$

where $N(D_i)$ is the DSD, $\sigma(D_i)$ the radar cross section, D_i the rain drop equivolumetric diameter, $v_f(D_i)$ the rain drop fall velocity, θ the elevation angle and ζ the inertia correction, which is equal to 1 in case there is no inertia correction. The turbulence spectral width without inertia correction, σ_T , can be related to the EDR as [30]:

$$\sigma_T^2 = \frac{C\epsilon^{2/3}}{4\pi} I, \quad (35)$$

where C is a Kolmogorov constant, ϵ the EDR and I an elaborate integral for which we refer to White *et al.* [30]. The equivalent reflectivity factor $Z(v_1, v_2)$ in the velocity interval $[v_1, v_2]$, which can be used to calculate the power Doppler spectrum, is equal to:

$$Z(v_1, v_2) = \sum_i N(D_i)\sigma(D_i)f(D_i, v_1, v_2) \quad (36)$$

where $f(v_1, v_2, D_i)$ is the fraction of Doppler velocities that are between v_1 and v_2 . It can be calculated with the inverse cumulative normal distribution function $F^{-1}(p|\mu, \sigma)$ with mean μ and standard deviation σ as:

$$f(v_1, v_2, D_i) = F^{-1}(v_2|v_f(D_i) \sin \theta, \zeta_T(D_i)\sigma_T) - F^{-1}(v_1|v_f(D_i) \sin \theta, \zeta_T(D_i)\sigma_T). \quad (37)$$

The advantage of this formulation is that the fall velocity and cross section are still in symbolic form and the choice for cross sections and fall velocities calculations is unconstrained. It is general enough to extend it to polarimetric radar observables and/or use Mie cross sections, e.g. cross sections from Mishchenko [31]. However these new formulations do not solve the problem as the radar observables typically do not carry sufficient information on the DSD and additional constraints for the retrieval are required. An example of such constraints are linked DSD parameters, which are used in radar DSD retrievals

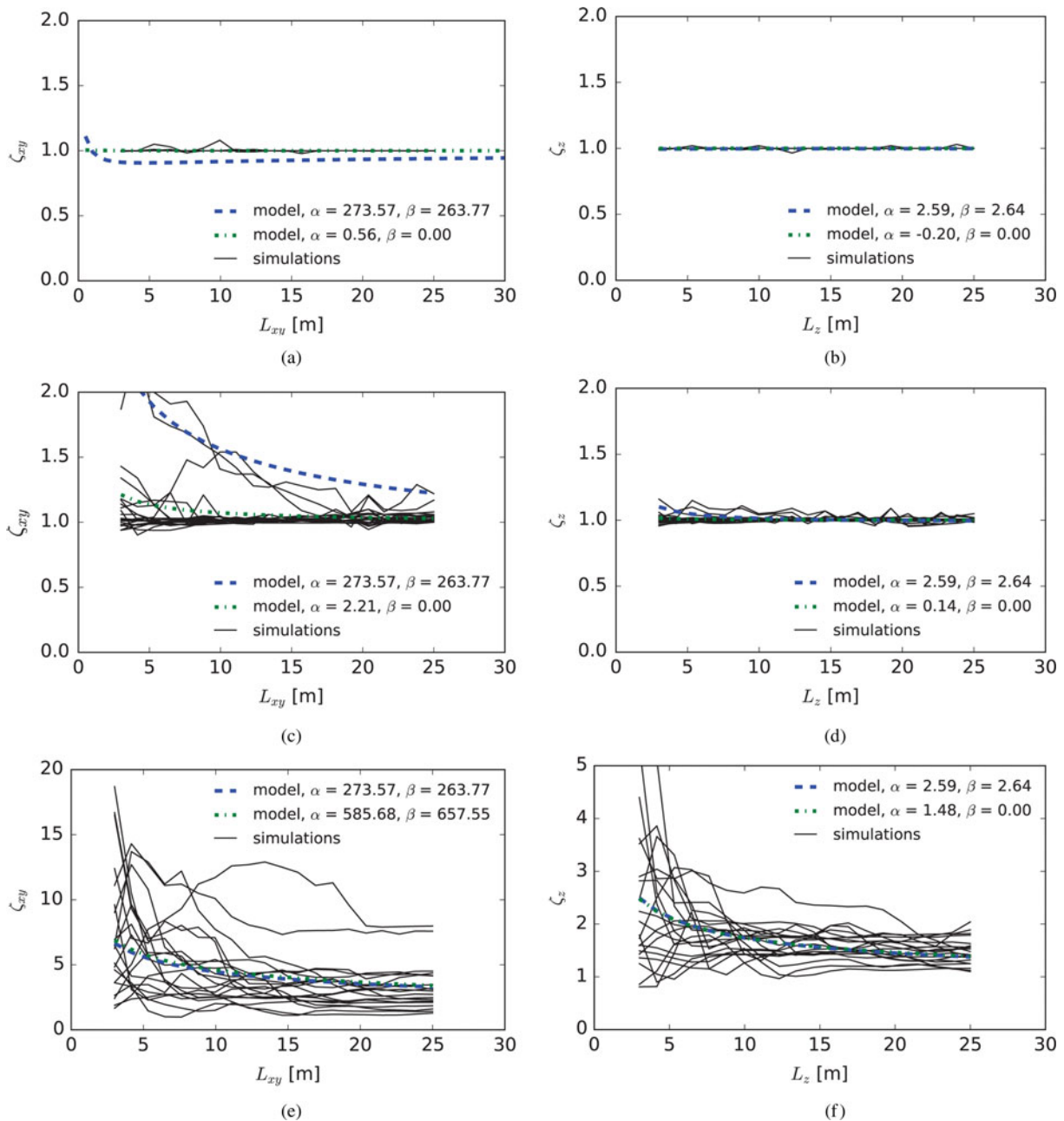


Fig. 4. Calculation of inertia factor $\zeta_{,i}$ for different simulations i , that have a random position in the 3-D wind field simulation. The calculations are done for different equivolumetric rain drop diameters D and for different looking directions. On the x -axis the length of the line $L_{,i}$ is varied, on which 100 equidistant points are put to calculate the Doppler velocity variance. (a) $D = 0.1$ mm, x -direction (b) $D = 0.1$ mm, z -direction, (c) $D = 0.5$ mm, x -direction (d) $D = 0.5$ mm, z -direction, (e) $D = 4$ mm, x -direction (f) $D = 4.0$ mm, z -direction.

[32]. However, constraints that are typically used for weather radars are limited to radars with a low elevation angle and cannot be applied in a general context. The application of the new radar forward model, including finding appropriate constraints for a specific radar configuration, is part of future research.

VI. CONCLUSION

In this paper rain drop inertial parameters were derived from fundamental physical laws. To achieve this the equations

of motion for a rain drop were solved to analytical solutions for the “sudden jump case” from which the rain drop inertial parameters can be defined. It became clear that the inertia effect is anisotropic, i.e. has a different behavior in the x/y - and z -direction. A new model is proposed to account for inertia in radar-based turbulence retrieval techniques. This model also accounts for the radar elevation and the changing scales, for which rain drops are sensitive. In this model for inertia correction dimensionless parameters are introduced that allow for model tuning. Although the simulations suggest certain preferable tuning values, more research is required to obtain the right tuning parameters. Mathematical

relations were given for the implementation of the inertia correction model in a generalized way for radar-based retrieval techniques.

ACKNOWLEDGEMENTS

This work was supported by the EU in the framework of the EU FP7 program, the UFO project. The authors also acknowledge three anonymous reviewers for their helpful comments.

REFERENCES

- [1] Spalart, P.R.: Airplane trailing vortices. *Annu. Rev. Fluid Mech.*, **30** (1) (1998), 107–138.
- [2] Barbaresco, F. et al.: Wake vortex detection, prediction and decision support tools in SESAR program. 2013 IEEE/AIAA 32nd Digital Avionics Systems Conf., 2013, 6B1–1–6B1–15.
- [3] Holzäpfel, F.: Probabilistic two-phase aircraft wake-vortex model: further development and assessment. *J. Aircr.*, **43** (3) (2006), 700–708.
- [4] Barbaresco, F. et al.: Eddy Dissipation Rate (EDR) retrieval with ultra-fast high range resolution Electronic-Scanning X-band airport radar: Results of European FP7 UFO Toulouse Airport trials, 2015.
- [5] Oude Nijhuis, A.C.P.; Unal, C.M.H.; Krasnov, O.A.; Russchenberg, H.W.J.; Yarovoy, A.: Outlook for a new wind field retrieval technique: The 4D-Var wind retrieval. In *Int. Radar Conf.*, 2014, 1–6.
- [6] Bringi, V.N.; Chandrasekar, V.: *Polarimetric Doppler Weather Radar: Principles and Applications*, Cambridge University Press, Cambridge, UK, 2001.
- [7] Doviak, R.J.; Zrnic, D.S.: *Doppler Radar and Weather Observations*, 2nd ed., Academic Press, San Diego, 1993.
- [8] Mishchenko, M.I.; Travis, L.D.; Lacis, A.A.: *Scattering, Absorption, and Emission of Light by Small Particles*, Cambridge University Press, Cambridge, UK, 2002.
- [9] Pope, S.B.: *Turbulent Flows*, Cambridge University Press, Cambridge, UK, 2000.
- [10] Brewster, K.A.; Zrnic, D.S.: Comparison of eddy dissipation rates from spatial spectra of Doppler velocities and Doppler spectrum widths. *J. Atmos. Ocean. Technol.*, **3** (3) (1986), 440–452.
- [11] Yanovsky, F.J.; Russchenberg, H.W.J.; Unal, C.M.H.: Retrieval of information about turbulence in rain by using Doppler-polarimetric Radar. *IEEE Trans. Microw. Theory Tech.*, **53** (2) (2005), 444–450.
- [12] O'Connor, E.J. et al.: A method for estimating the turbulent kinetic energy dissipation rate from a vertically pointing Doppler lidar, and independent evaluation from balloon-borne in situ measurements. *J. Atmos. Ocean. Technol.*, **27** (10) (2010), 1652–1664.
- [13] Chan, P.W.: Generation of an eddy dissipation rate map at the Hong Kong International Airport based on Doppler lidar data. *J. Atmos. Ocean. Technol.*, **28** (1) (2011), 37–49.
- [14] Bohne, A.R.: Radar detection of turbulence in precipitation environments. *J. Atmos. Sci.*, **39** (8) (1982), 1819–1837.
- [15] Frisch, A.S.; Strauch, R.G.: Doppler radar measurements of turbulent kinetic energy dissipation rates in a Northeastern Colorado convective storm. *J. Appl. Meteorol.*, **15** (9) (1976), 1012–1017.
- [16] Hocking, W.K.: Observation and measurement of turbulence in the middle atmosphere with a VHF radar. *J. Atmos. Terr. Phys.*, **48** (7) (1986), 655–670.
- [17] Shupe, M.D.; Brooks, I.M.; Canut, G.: Evaluation of turbulent dissipation rate retrievals from Doppler cloud radar. *Atmos. Meas. Tech.*, **5** (6) (2012), 1375–1385.
- [18] Yanovsky, F.J.; Prokopenko, I.G.; Prokopenko, K.I.; Russchenberg, H.W.J.; Lighthart, L.P.: Radar estimation of turbulence eddy dissipation rate in rain. In *IEEE Int. Symp. on Geoscience and Remote Sensing*, volume **1**, 2002, 63–65.
- [19] Brandes, E.A.; Zhang, G.; Vivekanandan, J.: An evaluation of a drop distribution-based polarimetric radar rainfall estimator. *J. Appl. Meteor.*, **42** (5) (2003), 652–660.
- [20] Unal, C.: High-resolution raindrop size distribution retrieval based on the Doppler spectrum in the case of slant profiling radar. *J. Atmos. Ocean. Technol.*, **32** (6) (2015), 1191–1208.
- [21] Yanovsky, F.J.; Turenko, D.M.; Oude Nijhuis, A.C.P.; Krasnov, O.A.; Yarovoy, A.: A new model for retrieving information about turbulence intensity from radar signal. In *2015 IEEE Symp. on Signal Processing*, June 2015, 1–6.
- [22] Rogers, R.R.; Tripp, B.R.: Some radar measurements of turbulence in snow. *J. Appl. Meteor.*, **3** (5) (1964), 603–610.
- [23] Yanovsky, F.J.: Simulation study of 10 GHz radar backscattering from clouds, and solution of the inverse problem of atmospheric turbulence measurements. In *3rd Int. Conf. Computer Electromagnetic (CEM 96)*, volume **1996**, IEE, 1996, 188–193.
- [24] Yanovsky, F.J.: Doppler-polarimetric retrieval of rain rate and turbulence intensity in precipitation. In *Proc. Int. Conf. Mathematical Methods in Electromagnetic Theory, MMET '02*, volume **1**, Kiev, 2002, 281–286.
- [25] Khvorostyanov, V.I.; Curry, J.A.: Fall velocities of hydrometeors in the atmosphere: refinements to a continuous analytical power law. *J. Atmos. Sci.*, **62** (12) (2005), 4343–4357.
- [26] Beard, K.V.; Chuang, C.: A new model for the equilibrium shape of raindrops. *J. Atmos. Sci.*, **44** (11) (1987), 1509–1524.
- [27] Kolmogorov, A.N.: Dissipation of energy in the locally isotropic turbulence. *Proc. R. Soc. A Math. Phys. Eng. Sci.*, **434** (1890) (1991), 15–17.
- [28] Mann, J.: Wind field simulation. *Probabilistic Eng. Mech.*, **13** (4) (1998), 269–282.
- [29] Fang, M.; Doviak, R.J.: Coupled contributions in the Doppler radar spectrum width equation. *J. Atmos. Ocean. Technol.*, **25** (12) (2008), 2245–2258.
- [30] White, A.B.; Latatis, R.J.; Lawrence, R.S.: Space and time filtering of remotely sensed velocity turbulence. *J. Atmos. Ocean. Technol.*, **16** (12) (1999), 1967–1972.
- [31] Mishchenko, M.I.: Calculation of the amplitude matrix for a nonspherical particle in a fixed orientation. *Appl. Opt.*, **39** (6) (2000), 1026.
- [32] Brandes, E.A.; Zhang, G.; Vivekanandan, J.: Comparison of polarimetric radar drop size distribution retrieval algorithms. *J. Atmos. Ocean. Technol.*, **21** (4) (2004), 584–598.



Albert C.P. Oude Nijhuis is a Ph.D. student at the Delft University of Technology. He received his M.Sc. degree in Meteorology and Physical Oceanography at the University of Utrecht in 2012. He worked as a satellite remote sensing researcher at the Royal Dutch Meteorological Institute (KNMI). He worked on improvements for the OMI total ozone column DOAS technique and for the ISOTROP project on satellite retrieval error estimation of e.g. tropospheric NO₂ for the new generation of European Sentinel

research satellites. In January 2013 he started as a Ph.D. candidate at the Delft University of Technology, working on new retrieval methods for wind and turbulence parameters by using radar and lidar observations.



Felix J. Yanovsky received his Engineering (M.S.) degree from the National Aviation University (NAU), Kiev, Ukraine, Ph.D. degree from the Moscow State Technical University (MSTUCA), and two D.Sc. (habilitation) degrees from NAU and MSTUCA. Currently he is Full Professor and the Head of Electronics Department at NAU. His research

achievements are in radar and remote sensing, Doppler polarimetry, signal processing, math modeling, multi-parametric, and adaptive methods. He is the author or co-author of more than 400 scientific papers, 10 books, and 40 invention patents. He is EuMA Member and IEEE Fellow. He served as the Chairman, Section organizer or TPC member of numerous International Conferences including EuMW; elected as Academician of Science Academies in Ukraine, USA, and Russia. In 1996 he was awarded as the State Prize Winner of Ukraine in the field of Science and Technology. He is elected as IEEE Ukraine Section Chair for 2016–2017.



Oleg A. Krasnov received his M.S. degree in Radio Physics from Voronezh State University, Russia, in 1982, and the Ph.D. degree in radiotechnique from the National Aerospace University Kharkov Aviation Institute, Ukraine, in 1994. In 1999 Dr. Krasnov joined the International Research Center for Telecommunications and Radar (IRCTR), TU Delft.

Since 2009 he is a senior researcher at the Microwave Sensing, Signals and Systems (MS3) section of the Faculty of Electrical Engineering, Mathematics, and Computer Science (EEMCS) at Delft University of Technology, and became an Universitair Docent (Assistant Professor) there in 2012. His research interests include radar waveforms, signal and data processing algorithms for polarimetric radars and distributed radar systems, multi-sensor atmospheric remote sensing, optimal resource management of adaptive radar sensors and distributed systems. He served as the Secretary of the 9th European Radar Conference (EuRAD2012), Amsterdam, the Netherlands.



Christine M.H. Unal After a master in Physics, she received the D.E.A. degree in Physics for Remote Sensing (University of Paris, 1987). She joined the Delft University of Technology in 1988 where she is a research scientist. She was first at the International Research Center for Telecommunications and Radar and from 2012 at the department

of Geoscience and Remote Sensing and at the Climate Institute. She started to focus on radar polarimetric calibration

and radar spectral polarimetry (quasi simultaneous Doppler spectra of polarimetric measurements, their processing and their interpretation). From 2003, she applied this expertise to enhance the processing of atmospheric echoes. Since 2012, her current research interests are: weather/atmospheric radar signal processing and searching for new retrieval techniques to estimate microphysical and dynamical properties of precipitation using ground-based radars.



Herman W.J. Russchenberg is Director of the TU Delft Climate Institute and Head of the Department of Geoscience and remote Sensing. He is a specialist in remote sensing of clouds and precipitation with ground-based radar, lidar and microwave radiometry. He is experienced in theoretical as well experimental research of the scattering

process and the retrieval of geo-physical parameters from radar and lidar measurements. He is one of the leading scientists of the Cabauw Experimental Site for Atmospheric Research.



Alexander G. Yarovoy (FIEEE' 2015) graduated from the Kharkov State University, Ukraine, in 1984 with the Diploma with honor in radiophysics and electronics. He received the Candidate Phys. & Math. Sci. and Doctor Phys. & Math. Sci. degrees in radiophysics in 1987 and 1994, respectively. In 1987 he joined the Department of Radiophysics

at the Kharkov State University as a Researcher and became a Professor there in 1997. From September 1994 through 1996 he was with Technical University of Ilmenau, Germany as a Visiting Researcher. Since 1999 he is with the Delft University of Technology, the Netherlands. Since 2009 he leads there a chair of Microwave Sensing, Systems and Signals. His main research interests are in ultra-wideband microwave technology and its applications (in particular, radars) and applied electromagnetics (in particular, UWB antennas). He has authored and co-authored more than 250 scientific or technical papers, four patents, and 14 book chapters.